

MULTI-SITE OBSERVATIONS OF δ SCUTI STARS 7 AQL AND 8 AQL (A NEW δ SCUTI VARIABLE): THE TWELFTH STEPPI CAMPAIGN IN 2003

L. FOX MACHADO¹, E. MICHEL², F. PÉREZ HERNÁNDEZ^{5,6}, J.H. PEÑA³, Z.P. LI⁴, M. CHEVRETON², J.A. BELMONTE⁵, M. ÁLVAREZ¹, L. PARRAO³, M.-A. DUPRET², S. PAU², A. FERNÁNDEZ², J.P. MICHEL², R. MICHEL¹, A. PANI¹

Draft version February 5, 2008

ABSTRACT

We present an analysis of the pulsation behaviour of the δ Scuti stars 7 Aql (HD 174532) and 8 Aql (HD 174589) – a new variable star – observed in the framework of STEPPI XII campaign during 2003 June–July. 183 hours of high precision photometry were acquired by using four-channel photometers at three sites on three continents during 21 days. The light curves and amplitude spectra were obtained following a classical scheme of multi-channel photometry. Observations in different filters were also obtained and analyzed. Six and three frequencies have been unambiguously detected above a 99% confidence level in the range $190\ \mu\text{Hz}$ – $300\ \mu\text{Hz}$ and $100\ \mu\text{Hz}$ – $145\ \mu\text{Hz}$ in 7 Aql and 8 Aql respectively. A comparison of observed and theoretical frequencies shows that 7 Aql and 8 Aql may oscillate with p modes of low radial orders, typical among δ Scuti stars. In terms of radial oscillations the range of 8 Aql goes from $n = 1$ to $n = 3$ while for 7 Aql the range spans from $n = 4$ to $n = 7$. Non-radial oscillations have to be present in both stars as well. The expected range of excited modes according to a non adiabatic analysis goes from $n = 1$ to $n = 6$ in both stars.

Subject headings: techniques:photometric – stars: individual: HD 174532 – stars: individual: HD 174589 – stars: oscillations– δ Scuti.

1. INTRODUCTION

Stellar oscillations provide a powerful tool for studying the interiors of the stars since the mode frequencies depend on the properties of the star and give strong constraints on stellar models and hence evolution theories. However, the observations of stellar pulsations require extensive data sets in order to achieve accurate frequencies and to avoid the side-lobes in the amplitude spectrum caused by the daily cycle. Great efforts are made to optimize the observational coverage of seismological observations, both from the ground via multisite coordinated campaigns (e.g. STEPPI [Michel et al. 2000], DSN [Breger et al. 1999]) and from space, where missions like COROT (Baglin 2003, Michel et al. 2005), will bring a close to a 100% observational coverage.

In the last two decades the STEPPI network (Stellar PHotometry International) has been engaged in a long-term program aimed at improving our knowledge and description of the physical processes at work in the interior of δ Scuti stars. In the framework of STEPPI campaigns most of the δ Scuti stars within Praesepe and Pleiades clusters have been observed (e.g. Álvarez et al. 1998, Hernández et al. 1998a, Fox Machado et al. 2002, Li et al. 2004) and several theoretical interpretations have been realized

(e.g. Michel et al. 1999, Hernández et al. 1998b, Fox Machado et al. 2006).

The present campaign was devoted to the field star 7 Aql (HD 174532, SAO 142696, HIP 92501), a δ Scuti variable discovered in a systematic search and characterization of new variables, in preparation of the COROT mission (Poretti et al. 2003). The star 7 Aql has been cataloged as an evolved δ Scuti star with a low projected rotational velocity, of $v \sin i = 32\ \text{km s}^{-1}$. This star is located in the HR diagramme ($\log g = 3.8 \pm 0.1$ at $T_{\text{eff}} = 7400 \pm 100\ \text{K}$) in the ambiguous transition phase between core hydrogen burning and thick shell hydrogen burning. This phase is sensitive to the treatment of the core overshooting process. In addition to this, its low $v \sin i$ value makes it an interesting target for modelling and seismic interpretation, since it restricts the seismic analysis either to a star with an intrinsic low rotational velocity or to a faster rotator but with a low inclination i value. For evolved δ Scuti variables a very dense spectrum of excited modes is predicted (Dziembowski & Królikowska 1990).

The star 8 Aql (HD 174589, SAO 142706, HIP 92524) was chosen as a comparison star because it is the only bright star located close enough to 7 Aql to permit the simultaneous monitoring with the main target within the field of view of the photometer ($\approx 12' \times 16'$) and before this campaign it was supposed a constant star (Poretti et al. 2003).

Table 1 shows the main observational parameters corresponding to the target stars as taken from the SIMBAD database operated by CDS (Centre de Données astronomiques de Strasbourg) including the parallax measurements of HIPPARCOS. Using these values and a reddening of $E(b - y) = 0.004\ \text{mag}$ (Poretti et al. 2003) we estimate a magnitude $M_v = 1.32 \pm 0.10$ for 7 Aql and $M_v = 1.42 \pm 0.10$ for 8 Aql. The estimated absolute magnitudes are in good agreement with those expected

¹ Observatorio Astronómico Nacional, Instituto de Astronomía – Universidad Nacional Autónoma de México, Ap. P. 877, Ensenada, BC 22860, México

² Observatoire de Paris, LESIA, UMR 8109, F-92195 Meudon, France

³ Instituto de Astronomía – Universidad Nacional Autónoma de México, Ap. P. 70-264, México, D.F. 04510, México

⁴ Beijing Observatory, Chinese Academy of Sciences, Beijing, P.R. China

⁵ Instituto de Astrofísica de Canarias, E-38205 La Laguna, Tenerife, Spain

⁶ Departamento de Astrofísica, Universidad de La Laguna, Tenerife, Spain

for δ Scuti variables (Rodríguez & Breger 2001). Moreover, according to these magnitudes and colour indexes ($B - V$) it follows that both stars are located inside the δ Scuti instability strip.

2. OBSERVATIONS

The observations in this campaign were carried out over the period 2003 June 17–July 7. As has been done in previous STEPPI campaigns, we observed from three sites well distributed in longitude around the Earth: Observatorio de San Pedro Mártir (SPM, operated by UNAM), Baja California, Mexico; Xing Long Station (XL, operated by the Beijing Observatory), Heibe province, China; and Observatorio del Teide (OT, operated by the IAC), Tenerife, Spain. Thus, we are able to limit systematic gaps in the monitoring of the light curves of our target stars, avoiding the formation of strong aliasing through side lobes of the spectral window in the Fourier spectrum.

Table 2 gives the log of observations. Bad weather conditions at XL did not allow us to get more than three nights of data from this observatory. A total of 183 hours of useful data were obtained during 21 nights of observations from the three sites. The overlapping between observatories was negligible and the efficiency of the observations was 36% of the cycle, which is typical for a STEPPI campaign.

Four-channel photometers were used at all sites with interferometric blue filters ($\lambda \approx 4200 \text{ \AA}$, $\Delta\lambda \approx 190 \text{ \AA}$). The channels were used to monitor the star 7 Aql, 8 Aql and two adjacent sky background positions. At SPM, the fourth channel was used to monitor the star 7 Aql in a yellow filter ($\lambda \approx 5500 \text{ \AA}$, $\Delta\lambda \approx 400 \text{ \AA}$).

The data reduction is similar to that reported in previous STEPPI campaigns (for details see Álvarez et al. 1998). First, nightly time series corresponding to sky background were subtracted. Then, we computed the magnitude differences 7 Aql – 8 Aql and subtracted from every light curve each night a second order polynomial. This removed low-frequency trends that could affect the detection of the oscillation modes at higher frequencies. Finally we joined the data to produce one temporal series. The resulting differential light curves for three selected days are shown in the top panels of Fig. 1.

Since only a comparison star was considered we also analyzed the light curves of each star separately. The middle and bottom plots in Fig. 1 show examples of the individual light curves of 7 Aql and 8 Aql respectively. Here a second order polynomial was used for filtering the low frequency trends, mainly the harmonics of the day. As can be seen in Fig. 1, even in the case of non-differential photometry the oscillations in 7 Aql and 8 Aql are clearly inferred with the dominant period of 8 Aql longer than that of 7 Aql.

With the data obtained at SPM we produced three additional temporal series, namely, 1) 7 Aql in blue–8 Aql, 2): 7 Aql in yellow–8 Aql, and 3) 7 Aql in blue–7 Aql in yellow. Thus, we are able to search for phase shifts and amplitude ratios between the two stars. In this case the amplitude spectrum has been filtered by a parabola. The additional results obtained with these light curves will be presented in Sect. 4.3.

3. SPECTRAL ANALYSIS

The frequency peaks of the light curves considered in the previous section were obtained by performing a non linear fit to the data. However, to show the results and for obtaining initial estimates of the parameters, we have calculated amplitude spectra of the time series by computing iterative sine wave fits (ISWF; Ponman 1981). The figures discussed here correspond to this method.

The window function of the observations is shown in Figure 2. A one-day alias of 58% of the main lobe amplitude is present. The resolution as measured from the FWHM of the main lobe in the spectral window is $\Delta\nu = 0.84 \mu\text{Hz}$.

The amplitude spectrum of the differential light curve 7 Aql–8 Aql is plotted starting in the left top panel of Fig. 3 and continues downward and to the right. In order to decide which of the peaks present in the amplitude spectrum can be regarded as signal from the star, we follow Álvarez et al. (1998), where it was shown that 3.7 times the mean amplitude level in the spectrum, calculated in boxes of $100 \mu\text{Hz}$, can represent very well the 99% confidence level given by statistical tests. Similar criteria was used in early STEPPI articles (e.g. Michel et al. 1992, Fox Machado et al. 2002). This confidence level is plotted as a continuous line in Fig. 3.

The spectrum is analyzed with a standard pre-whitening method such that in each step the frequency peak with the largest amplitude is subtracted from the time series. The frequency, amplitude and phase of the pre-whitening peak is estimated simultaneously with the previously subtracted ones by performing a non linear fit to the original light curve. A new amplitude spectrum with all the fitted peaks subtracted from the light curve is obtained and a new confidence level computed. Applying the method until the whole spectrum is below the 3.7 signal-to-noise level, the frequency peaks which are, with a probability of 99%, due to the star’s pulsation are obtained. The process is illustrated in Fig. 3. It can be seen that the amplitude spectrum of the differential light curve 7 Aql–8 Aql shows a spread of high signal-to-noise peaks between $80 \mu\text{Hz}$ and $300 \mu\text{Hz}$. The mean noise level in the amplitude spectrum reaches $580 \mu\text{mag}$ at $150 \mu\text{Hz}$ and $230 \mu\text{mag}$ at $400 \mu\text{Hz}$.

As commented earlier, both stars are variable and hence it is also necessary to analyze the individual light curves. In order to diminish as much as possible the transparency fluctuations on the non-differential data we have only considered 18 nights of high photometric quality. During those nights not only the observing conditions were good but also no pointing and guiding problems were present. A least-squares fit to a parabola was applied and subtracted from every light curve each of the 18 nights. The resulting amplitude spectra of the non-differential light curves for 7 Aql and 8 Aql are plotted in Fig. 4. The resolution in this case is $\Delta\nu = 1.0 \mu\text{Hz}$. The high signal-to-noise peaks are concentrated between $190 \mu\text{Hz}$ and $300 \mu\text{Hz}$ in 7 Aql and between $100 \mu\text{Hz}$ and $170 \mu\text{Hz}$ in 8 Aql. Although the signal-to-noise ratio is smaller in these spectra as compared to the differential light curve, they are good enough to detect the oscillation frequencies due to each star as discussed below.

4. RESULTS

4.1. Detected frequencies

TABLE 1
OBSERVATIONAL PROPERTIES OF THE STARS OBSERVED IN THE STEPPI 2003 CAMPAIGN. THE DATA WAS TAKEN FROM SIMBAD DATABASE.

Star	HD	HIP	ST	V	$B - V$	$v \sin i$ (km s^{-1})	parallax mas	M_V
7 Aql	174532	92501	A2	6.9 ± 0.1	$+0.285 \pm 0.009$	32 ± 3	7.70 ± 0.80	$M_v = 1.32 \pm 0.10$
8 Aql	174589	92524	F2	6.1 ± 0.1	$+0.299 \pm 0.007$	105 ± 11	11.80 ± 0.78	$M_v = 1.42 \pm 0.10$

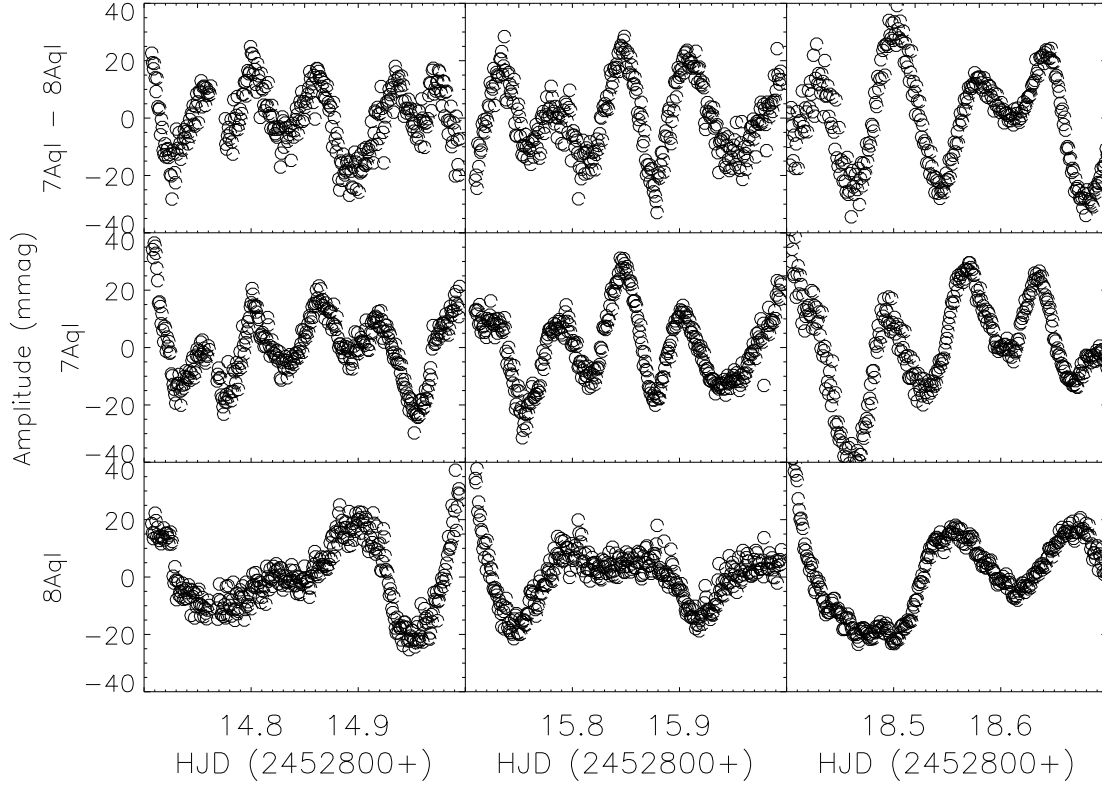


FIG. 1.— Examples of the light curves derived in the framework of STEPPI XII campaign. Data averaged every 62 seconds are represented by open circles. The three top plots correspond to the differential light curve 7 Aql–8 Aql, while the middle and bottom plots are light curves for the star indicated in each case. The time series were filtered by a second order polynomial.

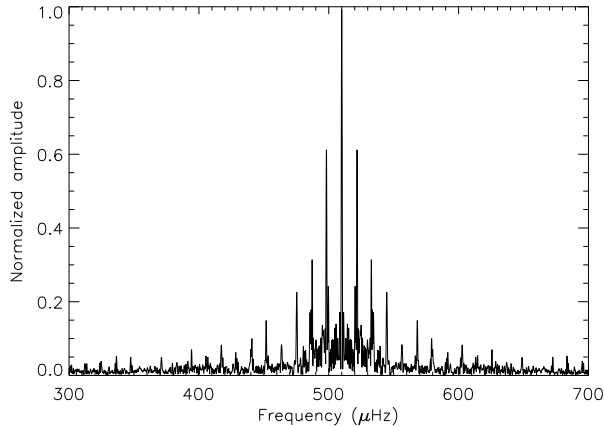


FIG. 2.— Spectral window in amplitude of STEPPI XII campaign. First side lobes are at 58% of the main lobe.

The results of the STEPPI XII multi-site campaign are summarized in Table 3, where the detected frequen-

cies with their corresponding amplitudes and phases are given. In total 9 peaks were detected in the spectrum of the differential light curve — ν_a and ν_b correspond respectively to 5 and 7 c/d and will not be considered hereafter.

In order to assign the peaks to a given star, we fit the individual light curves to sinusoidal functions with the frequencies fixed to the values obtained for the differential light curve. These frequencies are marked in Fig. 4 and the values of the amplitudes and phases resulting from the fit are given in Table 3, but only for the assigned star. Concerning this point, we note that the peaks of ν_2, ν_3 (in 7 Aql) and ν_8 (in 8 Aql) have $S/N > 4$ as indicated in Table 3 but also have a no significant amplitude in the other star's spectrum. Concerning ν_4, ν_6 and ν_9 they have $S/N > 3$ in the spectrum of 7 Aql and $S/N \leq 1.6$ in the other. On the other hand, the phases are in good agreement with those of the differential light curve.

A little more problematic can be ν_1, ν_5 and ν_7 since they are hidden in the noise. For ν_1 and ν_5 the fact that

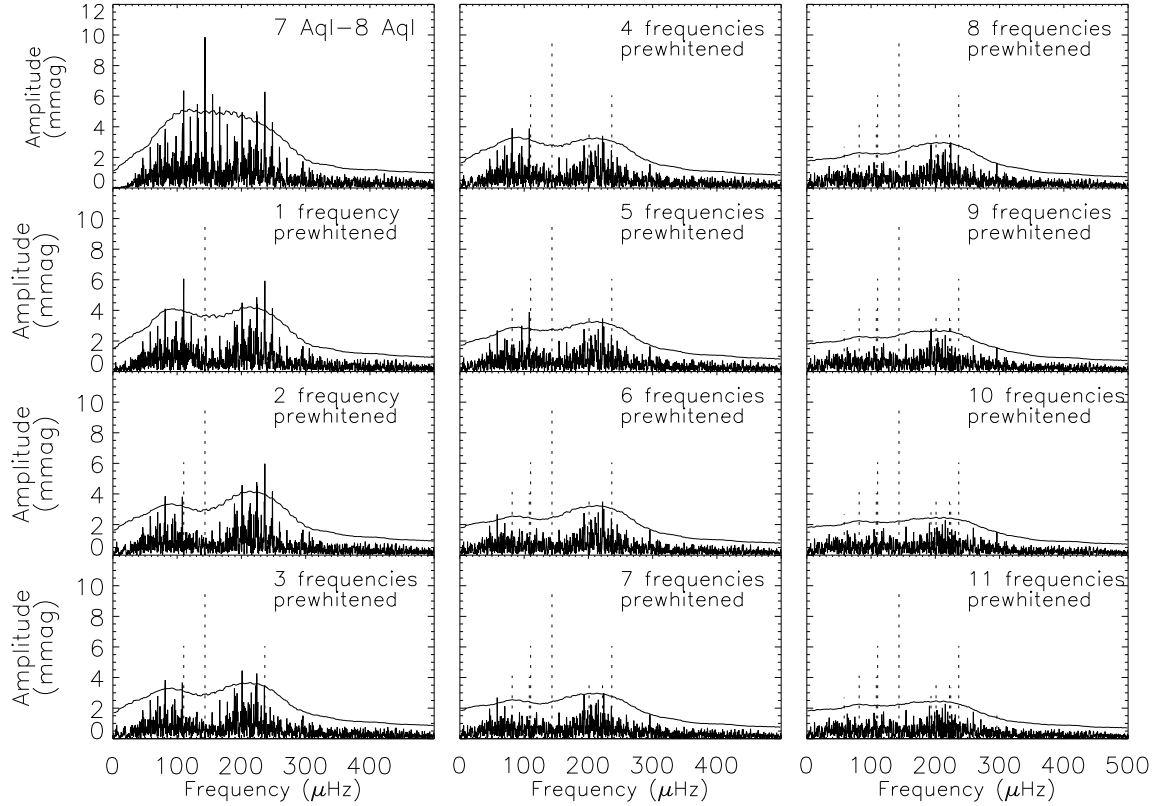


FIG. 3.— Pre-whitening process in the spectrum 7 Aql–8 Aql. In each panel, from top to bottom, one peak above the confidence level (continuous line) is selected and removed from the time series and a new spectrum is obtained. In each spectrum, the prewhitened frequencies are shown with vertical dot-dashed lines. The confidence levels are computed as indicated in the text.

TABLE 2
LOG OF OBSERVATIONS. OBSERVING TIME IS EXPRESSED IN MINUTES.

Day	Date 2003	HJD 2452800+	SPM	XL	OT
1	Jun 17	08	38	-	-
2	Jun 18	09	18	-	-
3	Jun 19	10	386	-	-
4	Jun 20	11	-	-	-
5	Jun 21	12	366	-	-
6	Jun 22	13	359	-	-
7	Jun 23	14	335	223	-
8	Jun 24	15	359	-	297
9	Jun 25	16	419	-	426
10	Jun 26	17	422	-	425
11	Jun 27	18	420	-	441
12	Jun 28	19	369	-	436
13	Jun 29	20	388	-	282
14	Jun 30	21	425	204	44
15	Jul 01	22	199	-	378
16	Jul 02	23	411	-	433
17	Jul 03	24	353	-	443
18	Jul 04	25	-	339	384
19	Jul 05	26	-	-	418
20	Jul 06	27	-	-	444
21	Jul 07	28	-	-	442
Total observing time			SPM	XL	OT
10967 (183 hours)			4908	766	5293

the phases agree with that of the differential data in one of the individual light curves and also because the signal in the other spectrum at those frequencies have $S/N \sim 1$ makes the identification secure.

As can be seen in Fig. 3 the peaks ν_6 and ν_7 are close frequency pair in the spectrum of the differential light curve. The existence of a residual frequency above 99% level, when one of them is removed during the prewhitening process, (see Fig. 3) gives some confidence that this pair of close oscillation frequencies are indeed intrinsic. In fact, they have a separation of $1.03 \mu\text{Hz}$ above the resolution limit ($0.84 \mu\text{Hz}$). We assigned ν_7 to 7 Aql because its phase in the spectrum of 7 Aql is in good agreement with that of the differential curve, in particular if one notes that both peaks ν_6 and ν_7 are close enough to each other to produce a beating phenomena.

From this analysis it follows that the frequency spectrum of both stars are not superposed. The 6 frequencies of 7 Aql are in the frequency range $195 \mu\text{Hz}$ – $300 \mu\text{Hz}$ and have amplitudes from 3 to 6 mmag. On the other hand the 3 peaks detected in 8 Aql are in the range $100 \mu\text{Hz}$ – $140 \mu\text{Hz}$ and with amplitudes from 4 to 10 mmag.

4.2. Discussion of the results

There is little information available in the literature about the oscillation behaviour of 7 Aql and 8 Aql. In particular, Poretti et al. (2003) did not find photometric variability in 8 Aql. For 7 Aql they reported a “peak-

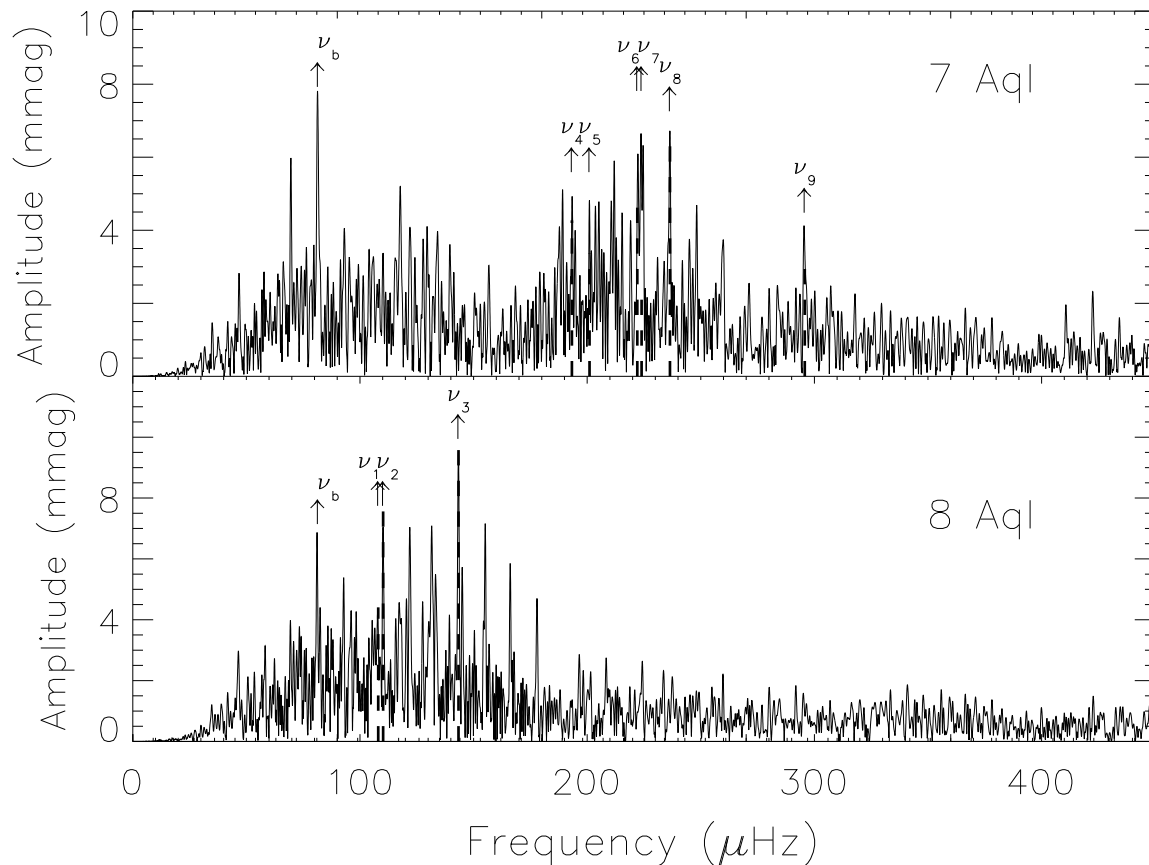


FIG. 4.— Amplitude spectrum derived from individual light curves filtered by a second order polynomial. The name of the star is indicated in each panel.

to-peak” amplitude of 25 mmag. While this has been enough to confirm the δ Scuti type variability in 7 Aql, the multi-periodicity of these oscillations have been confirmed only in this campaign.

From Table 3 it follows that the oscillation periods of 7 Aql and 8 Aql are within those found in others slightly evolved δ Scuti stars observed from the ground by means of multi-site networks (e.g Breger et al. 1999).

4.3. Observations in different filters

As was explained in Sect. 2 at San Pedro Mártir observatory two colour photometry was introduced in order to test the potential help this could bring on mode identification. Figure 5 shows the amplitude spectrum in different filters derived at SPM observatory. As it is known observations from a single site yield to a worse window function. In particular, in SPM observatory the side-lobes in the window function are at 88% of the main lobe. It is also important to note that at frequencies below $100 \mu\text{Hz}$ these spectra are dominated by the daily aliasing, mainly for the second one where we performed differential photometry with two stars in different filters.

In order to determine the differences in amplitude and phase between the different spectra a linear least-squares fit was performed to the SPM light curves with the frequencies fixed to the set listed in Table 3. The resulting phase differences and amplitude ratios between curves 7

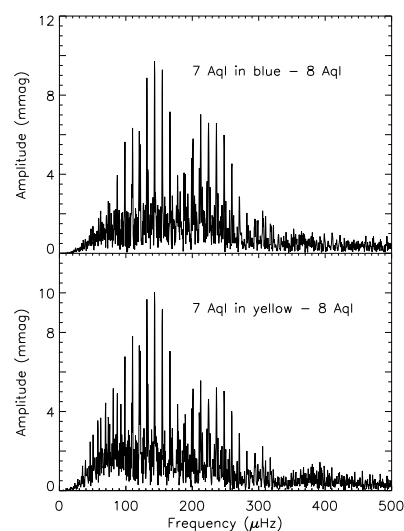


FIG. 5.— Amplitude spectrum derived from SPM light curves in different filters. The name of the curves are indicated in each panel.

TABLE 3

FREQUENCY PEAKS DETECTED ABOVE A 99% CONFIDENCE LEVEL IN THE LIGHT CURVE 7 Aql–8 Aql. THE ORIGIN OF φ IS AT HJD 2452809.71800. S/N IS THE SIGNAL-TO-NOISE RATIO IN AMPLITUDE AFTER THE PRE-WHITENING PROCESS. THE FORMAL ERRORS DERIVED FROM THE (NO WEIGHTING) NON LINEAR FIT ARE INDICATED. ALSO GIVEN ARE THE RESULTS OF THE FIT TO THE INDIVIDUAL LIGHT CURVES (AT FIXED FREQUENCIES). FOR THE PEAKS CORRESPONDING TO THE LIGHT CURVE OF 8 Aql A PHASE OF π HAVE BEEN ADDED TO HELP THE COMPARISON.

Series		ν	A	φ	S/N
		(μHz)	(mmag)	(rad)	
diff.	ν_a^*	58.15	2.7	–	–
	ν_b^*	81.39	4.1	–	–
	ν_1	108.04 ± 0.05	4.1 ± 0.1	-3.12 ± 0.12	6.9
	ν_2	110.20 ± 0.01	6.1 ± 0.1	-2.76 ± 0.02	10.2
	ν_3	143.36 ± 0.01	9.6 ± 0.1	$+2.72 \pm 0.01$	15.7
	ν_4	193.28 ± 0.02	2.8 ± 0.1	-1.53 ± 0.04	4.3
	ν_5	201.05 ± 0.01	3.8 ± 0.1	-2.83 ± 0.04	5.6
	ν_6	222.08 ± 0.01	3.6 ± 0.1	-2.32 ± 0.04	5.6
	ν_7	223.96 ± 0.02	3.4 ± 0.1	$+2.30 \pm 0.04$	5.2
	ν_8	236.44 ± 0.01	6.1 ± 0.1	-0.61 ± 0.02	9.9
	ν_9	295.78 ± 0.03	1.5 ± 0.1	$+1.19 \pm 0.08$	4.1
8 Aql	ν_1	108.04	4.4 ± 0.2	-2.91 ± 0.07	2.2
	ν_2	110.20	7.6 ± 0.2	-3.16 ± 0.03	5.1
	ν_3	143.36	9.8 ± 0.2	$+2.81 \pm 0.02$	7.9
7 Aql	ν_4	193.28	3.8 ± 0.2	-1.75 ± 0.05	3.6
	ν_5	201.05	3.0 ± 0.2	-2.83 ± 0.07	2.7
	ν_6	222.08	4.3 ± 0.2	-1.99 ± 0.05	3.9
	ν_7	223.96	2.2 ± 0.2	$+2.42 \pm 0.05$	2.0
	ν_8	236.44	5.8 ± 0.2	-0.56 ± 0.04	5.5
	ν_9	295.78	2.9 ± 0.2	$+1.14 \pm 0.09$	3.6

*5th and 7th harmonic of the day.

Aql in blue–8 Aql and 7 Aql in yellow–8 Aql are listed in Table 4 (columns 3–4). The given uncertainties correspond to the result of the no weighting fit. Since these uncertainties usually underestimate the true errors, it is not clear that the resulting differences between the two filters are real or are an artifact consequence of the bad coverage from a single site. To test this point we have also computed the spectrum of the light curve 7 Aql in blue–7 Aql in yellow. In this case, the extinction effects are not properly canceled and the daily aliasing dominate the spectrum. Even so we find some stellar signal above noise and the results of the linear fit at fixed frequencies are given in Table 4 (columns 5–7). At least for ν_8 we obtain a significant S/N , hence showing that the differences in amplitude and phase between the filters considered are indeed real.

The derived values of amplitude ratios and phase shift are discussed in the next section.

5. COMPARISON WITH THEORETICAL MODELS

In this section we will compute a set of representative models for our target stars to perform simple frequency comparisons, which will allow us to obtain some insights on their pulsation behaviour.

The computation of the theoretical evolutionary sequences and the calibration to the Johnson photometric system are explained in Fox Machado et al. (2006). In particular, we used the CESAM evolution code (Morel 1997) with input physics appropriate to δ Scuti stars and with a chemical initial composition of $Z = 0.02$ and $Y = 0.28$. Models with and without convective overshooting have been considered, in the latter case being the parameter $\alpha_{\text{ov}} = 0.2$. Rotating evolutionary models

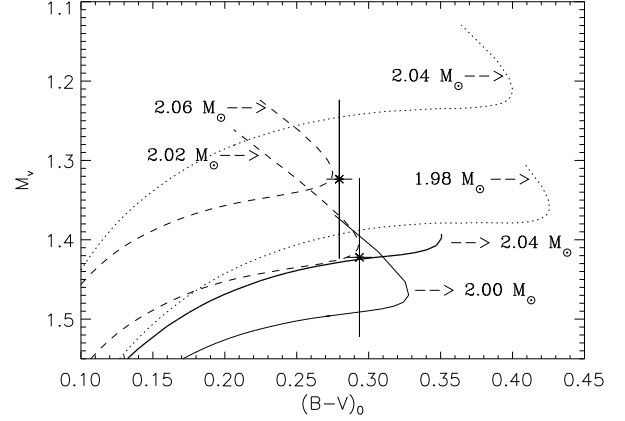


FIG. 6.— Colour-magnitude diagram showing the location of the target stars. The slightly cooler star is 8 Aql. Evolutionary sequences of non-rotating models with and without convective overshooting are shown by dotted and dashed lines respectively. The continuous lines are evolutionary sequence of models with no convective overshooting and initial rotation velocities of $v \simeq 121 \text{ km s}^{-1}$ (thin line) and $v \simeq 180 \text{ km s}^{-1}$ (thick line). The error bars give the position of the stars according to the uncertainties listed in Table 1.

were computed just for modelling 8 Aql since it is a rapid rotator ($v \sin i = 105 \text{ km s}^{-1}$).

Figure 6 shows the de-reddened position of the target stars in a colour-magnitude diagram. The slightly brighter star is 7 Aql. The error bars were already given in Table 1 and have been derived using HIPPARCOS data. The dashed and dotted lines are evolutionary sequences of non-rotating models with and without convective overshooting respectively, giving a range of masses suitable for 7 Aql. The continuous lines correspond to evolutionary tracks of rotating models of $2.00 M_{\odot}$ (thin line) and $2.04 M_{\odot}$ (thick line) which match approximately the observational position of 8 Aql. In this case, the initial rotational velocity used in each evolutionary sequence (121 km s^{-1} for $2.0 M_{\odot}$ and 180 km s^{-1} for $2.04 M_{\odot}$) is consistent with the high rotation rate observed in this star. Solid-body rotation, with conservation of global angular momentum during the evolution were assumed.

According to the models depicted in Fig. 6 our target stars could be in a similar evolutionary stage. In particular, their ages should be between 760 and 1100 Myr with a range of masses of $2.00 \pm 0.04 M_{\odot}$.

We now use these models to derive a range of radial orders of the target stars. The adiabatic eigenfrequencies were computed using the code FILOU (Tranh Minh et al. 1996, Suárez 2002). As can be seen in Table 3, some of the frequencies of 7 Aql (e.g. ν_1 and ν_2) and 8 Aql (e.g. ν_6 and ν_7) are so close that non radial oscillations need to be present. This is a common result among δ Scuti stars. However, at the evolutionary stage of our target stars the non radial oscillation modes develop a mixed character in the frequency range of interest making it difficult to assign radial orders to them without additional constraints. For this reason we prefer to give only the range of n associated to the radial oscillations, keeping in mind that p modes with $\ell > 0$ are present as well.

In Table 5 the possible range of radial orders of $\ell = 0$

TABLE 4

AMPLITUDE RATIOS A_v/A_y AND PHASE DIFFERENCES $\varphi_v - \varphi_y$ BETWEEN CURVES 7 AQL IN BLUE—8 AQL AND 7 AQL IN YELLOW—8 AQL. ALSO SHOWN ARE THE AMPLITUDES, PHASES AND SIGNAL-TO-NOISE RATIOS, S/N , OBTAINED FROM A FIT TO THE LIGHT CURVE 7 AQL IN BLUE—7 AQL IN YELLOW. THE QUOTED ERRORS ARE FROM THE NO WEIGHTING LEAST SQUARED FIT.

Frequency (μHz)	A_v/A_y	$\varphi_v - \varphi_y$ (radians)	A_{v-y} (mmag)	φ_{v-y} (radians)	S/N
ν_4 193.28	1.42 ± 0.15	-0.08 ± 0.11	—	—	1.6
ν_5 201.05	0.99 ± 0.08	-0.18 ± 0.08	—	—	1.3
ν_6 222.08	1.07 ± 0.06	$+0.01 \pm 0.06$	—	—	0.5
ν_7 223.96	1.64 ± 0.24	$+0.36 \pm 0.14$	1.31 ± 0.14	$+2.66 \pm 0.10$	2.8
ν_8 236.45	1.25 ± 0.05	-0.01 ± 0.04	1.39 ± 0.11	-0.67 ± 0.08	3.2
ν_9 295.78	1.76 ± 0.13	-0.19 ± 0.08	—	—	2.1

TABLE 5

FOR EACH OBSERVED FREQUENCIES THE POSSIBLE RANGE OF RADIAL ORDERS OF $\ell = 0$ MODES IS GIVEN. ALL THE MODELS HAVE $Z = 0.02$ AND $Y = 0.28$.

Obs. freq. (μHz)	$\alpha_{\text{ov}} = 0.00$		$\alpha_{\text{ov}} = 0.20$	
	$\ell = 0$		$\ell = 0$	
	n		n	
8 Aql				
$\nu_1 = 108.04$	1,2		1,2	
$\nu_2 = 110.19$	1,2		1,2	
$\nu_3 = 143.36$	2,3		2,3	
7 Aql				
$\nu_4 = 193.29$	4		4,5	
$\nu_5 = 201.05$	4		4,5	
$\nu_6 = 222.08$	5		5,6	
$\nu_7 = 223.96$	5		5,6	
$\nu_8 = 236.45$	6		6,7	
$\nu_9 = 295.78$	7		7	

modes for the observed frequencies is given. Here we have considered both models with and without convective overshooting. The theoretical frequencies of 8 Aql were computed up to second order in the rotation rate perturbative treatment. We note that the evolutionary sequences of rotating models with $\alpha_{\text{ov}} = 0.2$ are not shown in Fig. 6, but were computed with the same masses as indicated by the continuous lines.

Finally we have performed preliminary non-adiabatic computations corresponding to our target stars. The non-adiabatic pulsation models considered include the Time-Dependent Convection (TDC) treatment of (Gabriel 1996) and (Grigahcène et al. 2005). The probable evolutionary stage of the stars is shown in Fig. 6. In particular, for 7 Aql we have considered structure models with $M = 2M_{\odot}$, $T_{\text{eff}} = 7400$ K, $\log(L/L_{\odot}) = 1.387$, $X = 0.7$, $Z = 0.02$, $\alpha_{\text{ov}} = 0.2$ and different values of the mixing length parameter α (1.8, 1.5, 1 and 0.5).

The stability analysis shows that all the modes in the observed range of frequencies are predicted to be overstable, for 7 Aql and 8 Aql. The whole range of predicted overstable radial modes goes from $n = 1$ to $n = 6$.

As shown by Dupret et al. (2005), our TDC treatment allows a much more secure multi-colour photometric identification of the degree ℓ of the modes in δ Sct stars. However, in the case of 7 Aql, the observed error bars on the amplitudes and phases are too large to allow this identification. This is illustrated in Fig. 7, where the theoretical amplitude ratios and phases obtained with our TDC treatment for models with different ℓ and α

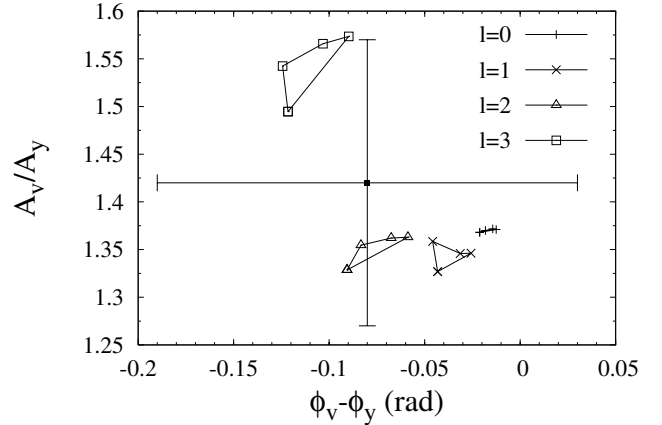


FIG. 7.— Theoretical amplitude ratios and phase differences compared with observations (big cross) for the mode ν_4 of 7 Aql. Each group of points related by lines corresponds to a different degree ℓ . Each point of a group corresponds to a model with given α (values: 0.5, 1, 1.5, 1.8).

are compared with observations (large cross).

6. CONCLUSIONS

We have presented the results obtained in the STEPHI XII multi-site campaign. The stars 7 Aql and 8 Aql were monitored for a period of 21 days during 2003 June–July. The analysis reveals that 8 Aql is a new δ Scuti variable.

The three-continent run allowed us to reach a low noise level ($\sim 230 \mu\text{mag}$ at $400 \mu\text{Hz}$) and a good spectral window (first side lobes at 58% of the main lobe in amplitude). The efficiency of the observations was 36% of the cycle. In fact our campaign represents the most extensive work on 7 Aql and 8 Aql in terms of the time, data points and observatories involved.

A long differential light curve of 7 Aql–8 Aql was obtained. High quality photometric nights of data were used to produce non-differential time series of each star. We have disentangled the peaks present in each star by comparing the amplitude and phases values of the non-differential time series to that of the differential light curve at fixed frequencies values. We have found that the frequency spectrum of both stars are not superposed. 7 Aql and 8 Aql have been found to be multi-periodic pulsators with at least six and three modes of oscillations respectively. The resulting amplitude spectra of non-differential and differential photometry do not shed any doubt on the results. Even so, we are considering new observations involving the faint comparison stars close to 7 Aql and 8 Aql in order to confirm the list of oscillation frequencies by means of ensemble photometry.

A comparison of observed and theoretical frequencies

of the radial modes reveals that pulsations in 7 Aql and 8 Aql can be due mostly to low order p modes with radial orders typical among δ Scuti stars. In particular, we have found that oscillation spectrum of 7 Aql and 8 Aql contain frequencies of radial modes with overtones up to $n = 7$ and $n = 3$ respectively. Non-radial oscillations must be present in both stars as well. A non-adiabatic analysis shows that the modes in the observed range of frequencies in 7 Aql and 8 Aql are theoretically overstable. The same range of radial orders were expected to be excited in both stars as opposite to what is found in the observations. In particular, the whole range of predicted overstable radial modes goes from $n = 1$ to $n = 6$ in both stars, whereas the observed frequency peaks in each star span over a more restricted range of consecutive radial orders between $n = 1$ to $n = 3$ (in 8 Aql) and between $n = 4$ to $n = 7$ (in 7 Aql).

This work has received financial support from the French CNRS, the Spanish DGES (AYA2001-1571, ESP2001-4529-PE and ESP2004-03855-C03-03), the Mexican CONACYT and UNAN under grant PAPIIT IN110102 and IN108106, the Chinese National Natural Science Foundation under grant number 10573023 and 10433010. Special thanks are given to the technical staff and night assistant of the Teide, San Pedro Mártir and Xing-Long Observatories and the technical service of the Meudon Observatory. The 1.5 m Carlos Sánchez Telescope is operated on the island of Tenerife by the Instituto de Astrofísica de Canarias in the Spanish Observatorio del Teide. This research has made use of the SIMBAD database operated at CDS, Strasbourg (France). We thank the anonymous referee for helping us to improve the manuscript.

REFERENCES

- Álvarez, M., et al. 1998, *A&A*, 340, 149
 Baglin, A. 2003, *AdSpR*, 31, 345
 Breger, M., et al. 1999, *A&A*, 349, 225
 Dupret, M.-A., et al. 2005, *MNRAS*, 361, 476
 Dziembowski, W. & Królikowska, M. 1990, *Acta Astron.*, 40, 19
 Fox Machado, L., et al. 2002, *A&A*, 382, 556
 Fox Machado, L., et al. 2006, *A&A*, 446, 611
 Grigahcène, A., et al. 2005, *A&A*, 434, 1055
 Gabriel, M. 1996, *Bull. Astron. Soc. of India*, 24, 233
 Hernández, M.M., et al. 1998a, *A&A*, 337, 198
 Hernández, M.M., et al. 1998b, *A&A*, 338, 511
 Li, Z.-P., et al. 2004, *A&A*, 420, 283
 Michel, E., et al. 2005, in *ASP Conf. Ser. 333, Tidal Evolution and Oscillations in Binary Stars*, ed. A. Claret, A. Giménez & J.-P. Zahn (San Francisco:ASP), 264
 Michel, E., et al. 1992, *A&A*, 255, 139
 Michel, E., et al. 2000, in *ASP Conf. Ser. 203, The Impact of Large-Scale Surveys on Pulsating Star Research*, ed. L. Szabados and D. W. Kurtz (San Francisco:ASP), 483
 Michel, E., et al. 1999, *A&A*, 342, 153
 Morel, P. 1997, *A&AS*, 124, 597
 Ponman T. 1981, *MNRAS*, 196, 543
 Poretti, E., et al. 2003, *A&A*, 406, 203
 Rodríguez, E., Breger, M. 2001, *A&A*, 366, 178
 Suárez J.C., 2002, Ph.D. Thesis, Sismologie d'étoiles en rotation. Application aux étoiles δ Scuti (Université Paris (Denis Diderot))
 Trinh Minh F., et al. 1996, in *IAU Symp. 181, Sounding solar and stellar interiors*, ed. J. Provost & F.X. Schmider, Poster Volume 4-18